nature communications

Article

https://doi.org/10.1038/s41467-024-55252-4

Sleep drive is coupled to tissue damage via shedding of *Caenorhabditis elegans* EGFR ligand SISS-1

Received: 15 July 2024

Accepted: 4 December 2024

Published online: 30 December 2024

Check for updates

Andrew J. Hill[1,3], Bryan Robinson[1], Jesse G. Jones[1], Paul W. Sternberg[2] & Cheryl Van Buskirk[1]

The benefits of sleep extend beyond the nervous system. Peripheral tissues impact sleep regulation, and increased sleep is observed in response to damaging conditions, even those that selectively affect non-neuronal cells. However, the 'sleep need' signal released by stressed tissues is not known. Sleep in the nematode *C. elegans* is independent of circadian cues and can be triggered rapidly by damaging conditions. This stress-induced sleep is mediated by neurons that require the Epidermal Growth Factor Receptor (EGFR) for their sleep-promoting function, but the only known *C. elegans* EGFR ligand, LIN-3, is not required for sleep. Here we describe SISS-1 (stress-induced sleepless), an EGF family ligand that is required for stress-induced sleep. We show that SISS-1 overexpression induces sleep in an EGFR-dependent, sleep neuron-dependent manner. We find that SISS-1 undergoes stress-responsive shedding by the ADM-4/ADAM17 metalloprotease, and that the ADM-4 site of action depends on the tissue specificity of the stressor. Our findings support a model in which SISS-1 is released from damaged tissues to activate EGFR in sleep neurons, identifying a molecular link between cellular stress and organismal sleep drive. Our data also point to a mechanism insulating this sleep signal from EGFR-mediated signaling during development.

Prolonged wakefulness is associated with perturbations of cellular homeostasis in the brain as well as in peripheral tissues[1–4]. Conversely, sleep is associated with the repair of cellular damage arising from wakefulness or from noxious conditions[5,6]. These observations provide insight into the benefits of sleep, including those that extend beyond the brain, and they suggest that tissues may respond to stress that accumulates during wakefulness by generating systemic sleep-promoting signals[7,8]. In the nematode *Caenorhabditis elegans*, exposure to damaging conditions induces a transient sleep state characterized by a cessation of feeding and a quickly-reversible suppression of movement and sensory responsiveness[9,10]. This stress-induced sleep (SIS) can be triggered by a variety of stimuli, including noxious heat, UV irradiation, high osmolarity, wounding, and exposure to pore-forming bacterial toxin[9–12]. SIS is not dependent on sensory perception of the noxious condition[12], suggesting that cellular damage itself initiates the SIS response. In support of this, UV stress-induced sleep (UV-SIS) is enhanced when DNA double-stranded break repair is compromised[12], and heat stress-induced sleep (heat-SIS) is enhanced when proteostasis is disrupted by mutation of the major chaperone *hsf-1*/HSF-1[12] or the E3 ubiquitin ligase *sel-11*/SEL-11[8]. Correspondingly, in *daf-21* mutants, predicted to have enhanced chaperone activity, heat-SIS is reduced[12].

Damage within a variety of tissues can trigger SIS. For example, wounding of the head, mid-body, or tail can induce sleep[12], as can intestine-specific damage from ingestion of pore-forming toxin[9]. Heat stress is predicted to have more widespread effects within the animal,

[1]Department of Biology, California State University Northridge, Northridge, CA, USA. [2]Division of Biology and Biological Engineering, California Institute of Technology, Pasadena, CA, USA. [3]Present address: Department of Molecular and Cell Biology, University of California Berkeley, Berkeley, CA, USA.
e-mail: cheryl.vanbuskirk@csun.edu

and accordingly, the enhanced heat-SIS that is observed in proteostasis-defective mutants appears to be attributable to disruption of homeostasis in multiple tissues[8,12].

Stress-induced sleep is not a behavioral consequence of widespread cell-autonomous dysfunction caused by cellular damage. Instead, SIS is mediated by two sleep-promoting interneurons – ALA and RIS – indicating that SIS is a programmed response to cellular stress[9,10,13]. The ALA neuron expresses a set of neuropeptides that execute the sub-behaviors of sleep, including cessation of feeding, locomotion, head movement, and sensory responsiveness[14]. Animals defective in ALA neuron specification are sleepless and impaired for survival compared to wild type after a severe exposure to heat stress[9,13], suggesting that the sleep state promotes cellular homeostasis. The RIS interneuron is a potential target of ALA neuropeptides during SIS, as ALA activation precedes RIS activation and RIS-defective animals fail to fully cease movement[13]. The Epidermal Growth Factor Receptor (EGFR) LET-23 is highly expressed in the ALA neuron[15] and is required for stress-induced sleep[9,10]. LET-23 is also expressed in the RIS neuron, where its activation may sensitize RIS to input from ALA[13]. Consistent with a role for EGFR signaling in sleep, transgenic overexpression of the *C. elegans* EGF family ligand LIN-3 promotes robust behavioral quiescence that requires LET-23 function within these sleep-promoting neurons[13,15]. While reduction of LIN-3 function has little impact on SIS[9], LIN-3 has nonetheless been considered the endogenous sleep-promoting EGF signal, as it is the only EGFR ligand that has been identified in *C. elegans*.

Here we describe SISS-1, a *C. elegans* EGFR ligand that exhibits stress-responsive shedding and is critically required for stress-induced sleep. We show that SISS-1 overexpression potently induces sleep in an EGFR-dependent and sleep neuron-dependent manner. We identify the SISS-1 sheddase as ADM-4, a metalloprotease orthologous to vertebrate ADAM17, and we show that the site of ADM-4 action varies with the type of damage used to trigger SIS. Our studies indicate that LIN-3 is not the only functional EGF family ligand in *C. elegans* and suggest that SISS-1/EGF is shed from damaged tissues to activate sleep-promoting neurons.

Results

The ADM-4 metalloprotease is necessary for stress-induced sleep

Stress-induced sleep (SIS) in *C. elegans* is dependent on the Epidermal Growth Factor Receptor (LET-23/EGFR)[9], and forced activation of LET-23 via overexpression of LIN-3/EGF promotes anachronistic sleep[15]. EGFR ligands are produced as transmembrane precursors that require proteolytic cleavage, or 'shedding,' for release of their growth factor ectodomain[16]. As such, we reasoned that activation of LET-23 in response to cellular stress should depend on ectodomain shedding of LIN-3, the only known *C. elegans* EGFR ligand[17,18]. *Drosophila* EGFR ligands are released by Rhomboid intramembrane proteases[19], whereas vertebrate EGF family ligands are shed by proteases of the ADAM (A Disintegrin And Metalloproteinase) family[20]. As certain vertebrate ADAMs are known to be activated by cellular stress[21], we considered the possibility that *C. elegans* ADAMs might be involved in stress-induced sleep. Using RNA-mediated interference we found that SIS was reduced in animals with impaired expression of *adm-4*, the *C. elegans* ortholog of vertebrate ADAM17/TACE (tumor necrosis factor alpha converting enzyme) (Supplementary Fig. 1a, b). ADAM17 cleaves dozens of transmembrane substrates, including various cytokines and EGF family ligands[22], and is activated by oxidative and osmotic stresses in mammalian cells[21]. To further investigate the role of ADM-4 in stress-induced sleep, we examined two *adm-4* mutants: *adm-4(ok265)*, a deletion spanning exons 9 through 13, as well as a CRISPR/Cas9 targeted allele, *sy1161*, harboring a STOP-IN cassette[23] in the 4th exon (Fig. 1a). We found that animals lacking ADM-4 are severely sleep-impaired following heat, UV, or Cry5B stress (Fig. 1b–d), as well as other stressors known to trigger sleep (Supplementary Fig. 1c–e). The *adm-4* SIS-defective phenotype is similar to that of *ceh-17(np1)* animals, which are impaired in the function of the sleep-promoting ALA neuron[9,24].

We reasoned that the requirement for ADM-4 in stress-induced sleep likely reflects a role in shedding LIN-3/EGF. LIN-3 overexpression (OE) from a heat-inducible promoter triggers a robust sleep state[15], and we predicted that this effect should rely on ADM-4 activity. We examined LIN-3(OE) sleep in *adm-4(sy1161)* animals, and we were surprised to find it unimpaired (Fig. 1e). While it is possible that ectopic LIN-3 overexpressed from the *hsp-16* promoter might be subject to non-physiological shedding, these data suggest that LIN-3 is not the sleep-relevant ADM-4 target. Further, unlike *lin-3* loss-of-function mutants[17], *adm-4* mutants are fully viable and fertile[25] and do not show defects in vulval development (Supplementary Fig. 1f), suggesting that ADM-4 is unlikely to be a LIN-3 sheddase in any context. Together our data indicate that ADM-4 acts upstream of EGFR activation during SIS but does not function to shed LIN-3/EGF, pointing to the existence of a yet-unidentified *C. elegans* EGFR ligand.

The SIS-defective mutant *csn20* reveals an EGF family ligand

In an EMS screen for SIS-defective mutants we identified *csn20*, a penetrant sleepless mutant with no other visible defects. SNP mapping and whole-genome sequencing showed that the causative mutation lies within an uncharacterized gene, F28E10.2, which we named *siss-1* for stress-induced sleepless. The gene encodes a predicted single-pass transmembrane protein with an extracellular EGF domain and an N-terminal immunoglobulin (Ig) fold[26] (Fig. 2a). Functional EGF domains participate in receptor binding via three loops formed by disulfide bonds among six highly conserved cysteines[16]. The *csn20* mutation is a Cys-to-Tyr substitution in the third of these cysteines (Fig. 2b), suggesting that the EGF domain is critical to SISS-1 function. Importantly, the *siss-1* gene contains an intron between the fourth and fifth cysteines (Fig. 2c), a near-invariant feature of EGF family ligands[27]. Multiple sequence alignment (Fig. 2b) and pairwise sequence comparisons (Supplementary Table 1) of EGF domains across taxa reveal relatively low similarity between SISS-1 and LIN-3, indicating that these *C. elegans* EGF family members are not related by a recent gene duplication.

Immunoglobulin and EGF domains are found together in the ectodomains of *Drosophila* Vein and human neuregulins NRG1 and NRG2 (Supplementary Fig. 2), and the impact of the Ig fold on EGF signaling appears to vary across phyla[28,29]. Like the neuregulins, SISS-1 lacks a signal sequence, and its transmembrane region likely serves as a reverse signal-anchor[30]. Two splice forms have been annotated for *siss-1*[18] with most sequenced RNAs corresponding to F28E10.2b, encoding a protein of 274 amino acids (Fig. 2d). A CRISPR deletion allele (*ve532*) spanning all *siss-1* exons (Fig. 2c) has been generated by the *C. elegans* Gene Knockout Consortium[31].

SISS-1 is required for stress-induced sleep and functions genetically upstream of EGFR

To confirm that SISS-1 is required for stress-induced sleep, we examined the *siss-1(ve532)* deletion allele. Like *csn20* mutants, *siss-1(ve532)* animals are severely defective in heat-SIS, UV-SIS, and Cry5B toxin-SIS (Fig. 3a–c). We examined the baseline activity of *siss-1* mutants, as certain mutations that confer hyperactivity are associated with SIS defects[32]. We found that *siss-1* mutants are not hyperactive, with wild-type baseline locomotion and pharyngeal pumping rates (Supplementary Fig. 3). Nonetheless, these animals fail to cease behaviors that are normally suppressed during SIS, including locomotion, head movement, and pharyngeal pumping. Thus, SISS-1 is required for stress-induced sleep, and a *siss-1* deletion phenocopies substitution of

https://doi.org/10.1038/s41467-024-55252-4

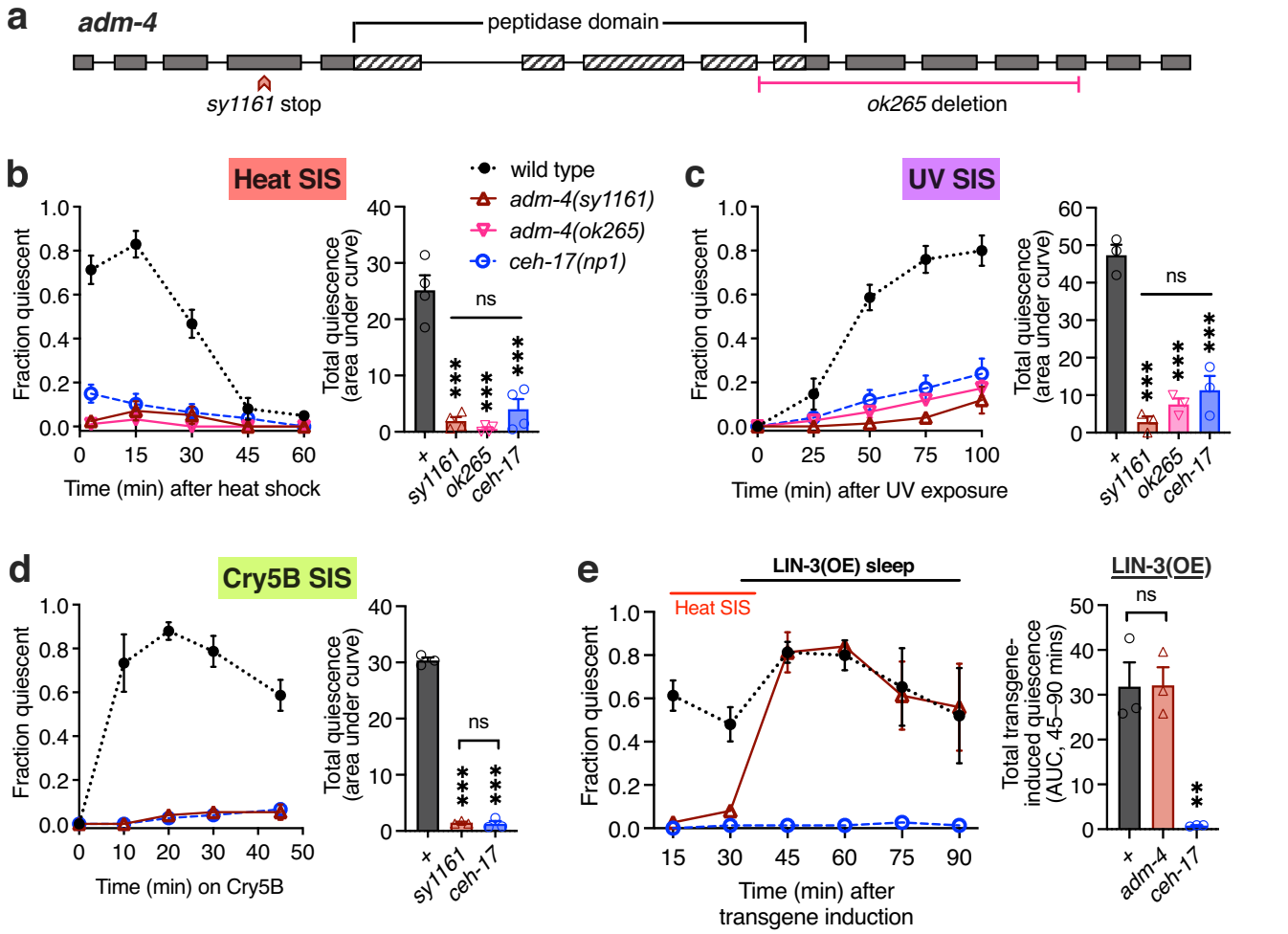

Fig. 1 | ADM-4 is required for SIS but does not act on LIN-3. a *adm-4* gene structure. Exons are depicted as solid boxes, and the peptidase domain is represented by striped segments. The alleles used in this study, CRISPR 'STOP-IN' *sy1161* and 846-bp deletion *ok265*, are annotated. **b**–**d** Fraction of animals that were quiescent over time (left) and total quiescence (area under curve (AUC), right) of wild type ("+," black trace), *adm-4(sy1161)* (maroon), *adm-4(ok265)* (pink), and ALA neuron-defective *ceh-17(np1)* (blue) animals: **b** following a 30-min 35 °C heat shock, **c** following a 50-sec UV-B exposure, or **d** during Cry5B exposure. **e** Time course of fraction quiescent (left) and total quiescence (AUC, right) of *syIs197;*+(black trace), *syIs197; adm-4(sy1161)* (maroon), and *syIs197; ceh-17(np1)* (blue) animals following a 20-min 35°C heat shock to induce expression of *lin-3*. The periods of quiescence caused by the heat itself (Heat SIS) and by the heat-induced expression of *lin-3* (LIN-3(OE) sleep) are labeled. The AUC calculation for transgene-induced quiescence excludes the first 45 min of the time course, to distinguish transgene-induced quiescence from Heat SIS. Each AUC data point represents one trial of 25 animals. All error bars represent SEM. ***$P < 0.0001$ vs. wild type, **$P = 0.0033$ vs. LIN-3(OE), ns = $P > 0.05$, One-way ANOVA with Tukey's multiple comparisons test. Source data are provided as a Source Data file.

a conserved cysteine within its EGF motif, indicating that the EGF motif of SISS-1 is critical to its function.

We reasoned that if SISS-1 normally functions to activate LET-23/EGFR, then LIN-3(OE) sleep should be intact in *siss-1* mutants. Alternatively, if SISS-1 plays a role in the development of sleep-promoting neurons, or functions at any step downstream of LET-23 activation, then LIN-3(OE) sleep should be impaired in *siss-1(lf)*, similar to ALA neuron-defective *ceh-17(lf)* mutants[15]. Using LIN-3(OE) to activate EGFR at the young adult stage, we observed robust sleep in *siss-1(lf)* animals, in stark contrast with *ceh-17(lf)* mutants (Fig. 3d). These data rule out a role for SISS-1 in the specification of neurons within the sleep circuit and are consistent with SISS-1 acting upstream of EGFR activation.

LIN-3/EGF does not appear to be required for stress-induced sleep

While conditional overexpression of LIN-3 promotes sleep[15], the requirement for LIN-3 in endogenous SIS is not well-defined. As LIN-3 and LET-23 are essential for viability and fertility, partial reduction-of-function alleles of *lin-3* and *let-23* have been examined for their impact on SIS[9]. While *let-23(rf)* animals show an overall reduction in sleep, *lin-3(rf)* animals show a mildly reduced peak but a longer duration of sleep, with no overall reduction relative to wild-type animals[9]. Further, RNAi against *let-23*, but not against *lin-3*, interferes with SIS (Supplementary Fig. 1a, b). The highly penetrant SIS defect of SISS-1 mutants indicates that there is little to no EGFR ligand redundancy during SIS. Nonetheless, we wished to investigate the potential contribution of LIN-3 to SIS more rigorously. To this end, we examined multiple forms of SIS in *lin-3(n1058)*, a strong reduction-of-function allele that confers sterility and partial lethality[33]. We examined two *lin-3(n1058)* strains, PS1378 and PS1595, that contain different second-site suppressors of *lin-3* sterility. Overall, our data indicate that LIN-3 is dispensable for stress-induced sleep but that these two strains harbor genetic modifiers that modulate SIS. Specifically, PS1378 animals display an abnormal heat-SIS profile but show no reduction in total sleep relative to wild-type, consistent with previous findings[9], and PS1595 animals show wild-type heat-SIS (Fig. 3e). UV-SIS is robust in PS1378 but impaired in PS1595; however, the observed defect in PS1595, which harbors a *dpy-20* mutation closely linked to *lin-3*, is phenocopied by a *dpy-20* mutation alone (Fig. 3f). Last, we observed robust Cry5B toxin-SIS in PS1595, while the PS1378 strain showed partial Cry5B resistance, a phenotype

https://doi.org/10.1038/s41467-024-55252-4

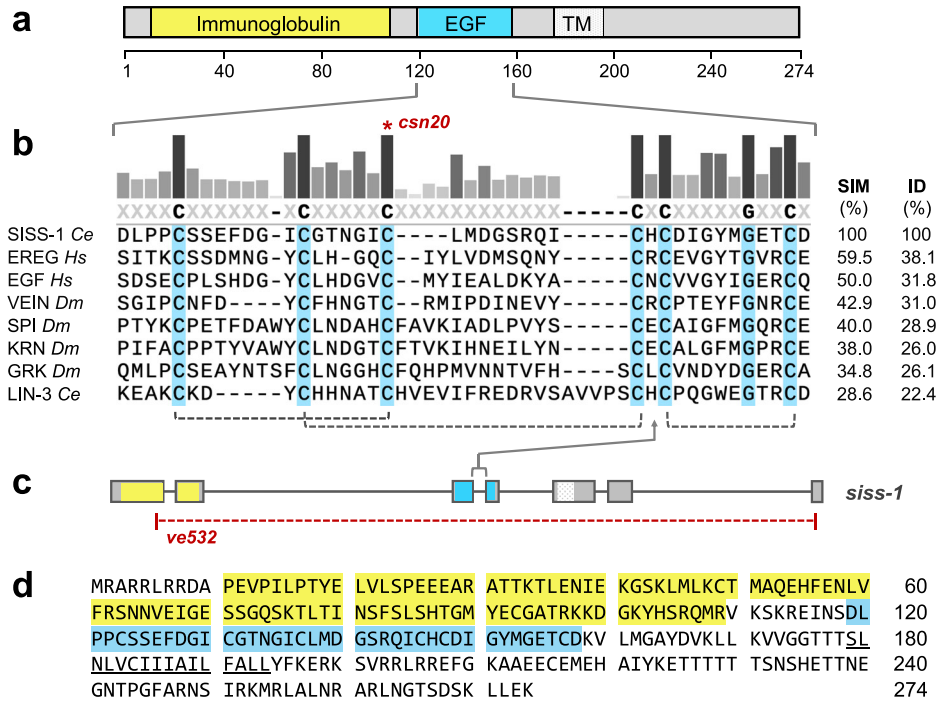

Fig. 2 | The *csn20* mutation disrupts the EGF motif of SISS-1. a The predicted SISS-1 protein contains an extracellular immunoglobulin fold (residues 11–109), an EGF domain (119–158), and a hydrophobic transmembrane anchor (178–194)[26]. **b** Multiple sequence alignment of the EGF domains of SISS-1 and selected EGFR ligands, shown in order of pairwise similarity to SISS-1 across the EGF domain: Epiregulin (EREG), Epidermal Growth Factor (EGF), Vein, Spitz (SPI), Keren (KRN), Gurken (GRK), and LIN-3. Consensus is shown at the top, and the *siss-1(csn20)* Cys-to-Tyr substitution is indicated by an asterisk. Disulfide bonds among invariant cysteines are indicated by dashed brackets at the bottom. **c** Exon structure of the predominant *siss-1* transcript F28E10.2b is shown with conserved placement of the EGF domain intron and the extent of the *siss-1(ve532)* deletion. **d** The amino acid sequence of the predicted SISS-1 protein, with immunoglobulin fold (yellow), EGF domain (blue) and transmembrane anchor (underlined) shown.

distinct from SIS-defective (Supplementary Fig. 4). We were able to outcross this Cry5B resistance, and the resulting *lin-3(n1058)* strain (CVB80) showed wild-type Cry5B-SIS (Fig. 3g). These data, along with the highly penetrant SIS defect of *siss-1* mutants, suggest that LIN-3 is dispensable for stress-induced sleep. However, as we are unable to assay a complete loss-of-function *lin-3* allele, and we have yet to examine all known SIS triggers, our data do not rule out the possibility that LIN-3 contributes to SIS in certain contexts. Unlike *lin-3* mutants, *siss-1* animals are viable and fertile and do not show defects in development of the hermaphrodite vulva or male spicules (Supplementary Fig. 1f). Our findings indicate that LIN-3 and SISS-1 play distinct roles in *C. elegans* development and behavior.

SISS-1 overexpression promotes sleep via EGFR

If SISS-1 is a functional EGFR ligand, we reasoned that SISS-1 overexpression (OE) should trigger sleep, similar to LIN-3(OE). Using the same method of inducible overexpression from a heat-responsive promoter used for LIN-3(OE)[15], we expressed the SISS-1 pro-protein at the young adult stage. We observed robust sleep beginning roughly 45 min after transgene induction (Fig. 4a). Like LIN-3(OE), SISS-1(OE)-induced sleep lasts several hours and includes a cessation of pharyngeal pumping and a complete but quickly reversible cessation of head and body movement. Importantly, the effect of SISS-1 expression is dependent on LET-23/EGFR (Fig. 4a, c). As complete loss of LET-23 is lethal, we used a partial reduction-of-function allele, *let-23(sy10)*, and observed partial suppression of SISS-1(OE) sleep. We further predicted that SISS-1(OE) sleep should require the ALA and RIS neurons, which each express LET-23 and mediate SIS. Animals lacking the homeobox transcription factor CEH-17 are defective in ALA function[24] as noted above, and animals lacking the AP2 transcription factor APTF-1 are defective in RIS function[34]. We found SISS-1(OE) sleep to be impaired in both *ceh-17(np1)* and *aptf-1(tm3287)* animals (Fig. 4b, c). ALA-defective animals were impaired in all aspects of SISS-1(OE)-induced sleep, while RIS-defective mutants were specifically impaired in movement quiescence (Supplementary Fig. 5), consistent with the functions of these neurons in SIS[9,13]. Thus, SISS-1(OE) triggers robust behavioral quiescence in a manner that depends on EGFR and on the EGFR-expressing neurons that mediate stress-induced sleep.

SISS-1 shedding is mediated by the ADM-4 metalloprotease

Given our findings that ADM-4 is required for SIS and acts upstream of EGFR activation (Fig. 1), we investigated whether ADM-4 functions as a SISS-1 sheddase. We first examined whether ADM-4 is required for the sleep-promoting effect of SISS-1 overexpression, and we found that *adm-4(lf)* mutants are indeed resistant to SISS-1(OE) sleep (Fig. 5a, c). We next reasoned that if this requirement for ADM-4 reflects its role as a sheddase, wherein it functions to release the EGF-containing ectodomain from membrane-bound pro-SISS-1, then expression of a constitutively secreted form of SISS-1 (sec-SISS-1) should circumvent the need for ADM-4. To test this prediction, we constructed a synthetic cDNA containing only the SISS-1 ectodomain, terminating 13 amino acids after the EGF domain. An N-terminal synthetic signal sequence[35] was added to target the protein to the secretory pathway, a function normally provided by the SISS-1 transmembrane region. We found that heat shock-induced expression of this secreted form of SISS-1 in wild-type animals produced robust sleep, similar to expression of full-length pro-SISS-1 but with an onset roughly 15 min earlier (Fig. 5a, b). This temporal difference may reflect differences in ER targeting, transit through the secretory pathway, or processing. Importantly, unlike pro-SISS-1 sleep, sec-SISS-1 sleep does not require ADM-4 (Fig. 5b, c). Thus, the requirement for ADM-4 in SISS-1-induced sleep can be bypassed with a constitutively secreted form of SISS-1. These data, together with the

https://doi.org/10.1038/s41467-024-55252-4

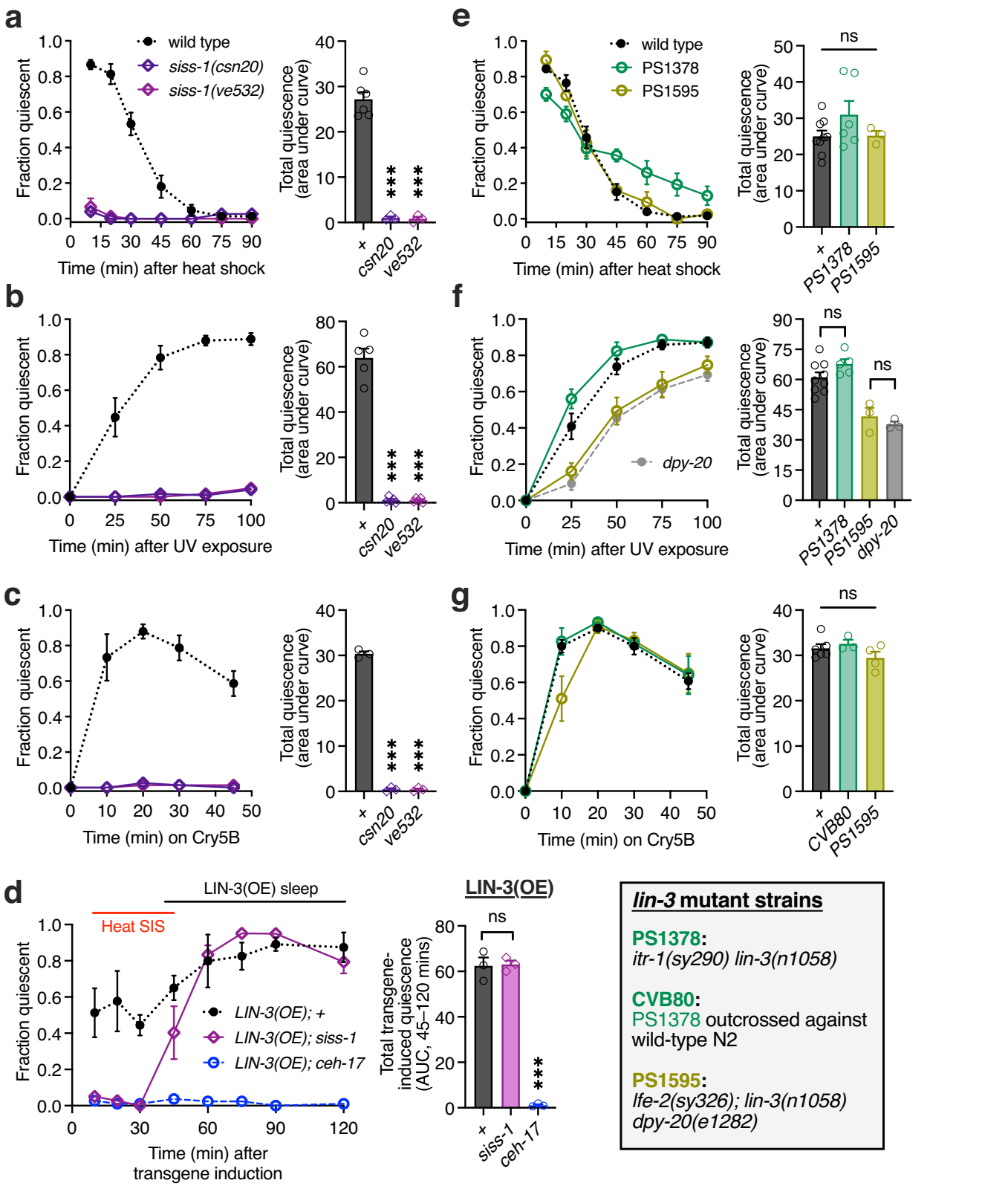

predicted function of ADM-4 as a membrane-bound metalloprotease, strongly implicate ADM-4 in SISS-1 ectodomain shedding. ADM-4 appears to function in the same manner as its vertebrate ortholog ADAM17, which has been shown to shed the ectodomains of a variety of substrates, including EGF family ligands[22,36]. Interestingly, long time courses of pro-SISS-1(OE) show an ADM-4-independent sleep bout roughly 3–5 h after transgene induction (Supplementary Fig. 6), an effect not observed during endogenous SIS, suggesting that SISS-1 can signal by another mechanism under certain conditions.

SISS-1 shedding is stress-responsive

Our data support a model wherein the ADM-4 metalloprotease sheds the ectodomain of SISS-1 in response to cellular stress. This model is consistent with observations in mammalian cells, which indicate that

https://doi.org/10.1038/s41467-024-55252-4

Fig. 3 | Stress-induced sleep requires SISS-1. a–**c** Fraction of animals that were quiescent over time (left) and total quiescence (area under curve (AUC), right) of wild type ("+," black trace), *siss-1(csn20)* (dark purple), and *siss-1(ve532)* (light purple) animals: **a** following a 30-min 35 °C heat shock, **b** following a 50-sec UV-B exposure, and **c** during Cry5B exposure. **d** Time course of fraction quiescent (left) and the total quiescence (AUC, right) of *LIN-3(OE) (syIs197);+* (black trace), *LIN-3(OE); siss-1(ve532)* (light purple), and *LIN-3(OE); ceh-17(np1)* (blue) animals following a 20-min 35 °C heat shock to induce expression of *lin-3*. The periods of quiescence caused by the heat itself (Heat SIS) and by the heat-induced expression of *lin-3* (LIN-3(OE) sleep) are labeled. The AUC calculation for transgene-induced quiescence excludes the first 45 min of the time course to distinguish transgene-induced quiescence from Heat SIS. **e**–**g** Same as in **a**–**c**, respectively, but for *lin-3* mutants, which are described below panel **g**. Each AUC data point represents one trial of 25 animals. All error bars represent SEM. ***$P < 0.0001$ vs. wild type in panels **a**–**c**, ***$P < 0.0001$ vs. *LIN-3(OE);+* in panel **d**, ns = $P > 0.05$, One-way ANOVA with Tukey's multiple comparisons test. Source data are provided as a Source Data file.

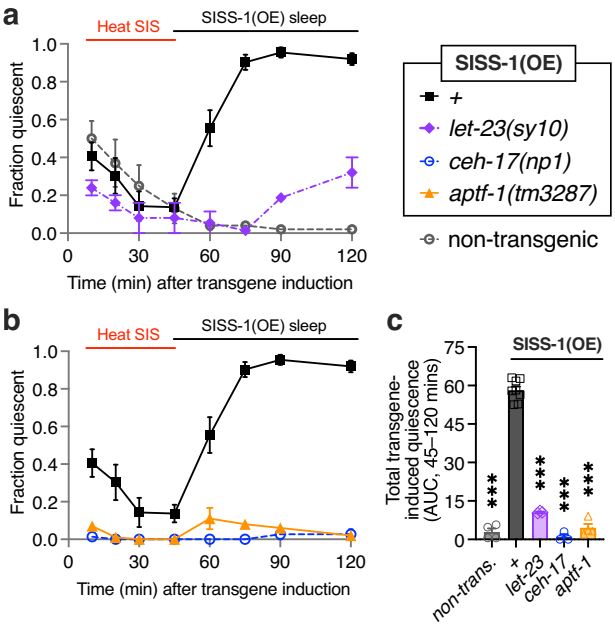

Fig. 4 | SISS-1 promotes sleep via EGFR, ALA and RIS. a, **b** Time course of fraction quiescent *pro-SISS-1(OE) (csnEx1);+* (black trace), *pro-SISS-1(OE); let-23(sy10)* (purple), *pro-SISS-1(OE); ceh-17(np1)* (blue), *pro-SISS-1(OE); aptf-1(tm3287)* (orange); and non-transgenic siblings of *pro-SISS-1(OE);+* (gray) animals during the 120 min following a 20-min 35 °C heat shock to induce expression of full-length *siss-1*. Panels **a** and **b** show different sets of genotypes for clarity. **c** Total transgene-induced quiescence (area under curve, AUC) for data shown in **a** and **b**. AUC calculation includes only the 45- to 120-min time points to distinguish transgene-induced quiescence from Heat SIS. Each AUC data point represents one trial of 25 animals. All error bars represent SEM. ***$P < 0.0001$ vs. *pro-SISS-1(OE);*, One-way ANOVA with Dunnett's multiple comparisons test. Source data are provided as a Source Data file.

ADAM17 is activated upon various forms of cellular damage[37–39]. We therefore wished to test whether SISS-1 shedding by ADM-4 is dependent on cellular damage. To this end, we examined the effects of expressing pro-SISS-1 and sec-SISS-1 with and without noxious heat stress. While the heat-responsive promoter driving the SISS-1 transgenes is active at temperatures as low as 29 °C[40], heat-SIS occurs following heat shocks above 30 °C, with more robust sleep observed with increasing temperature[9,10]. If SISS-1 shedding is cell stress-dependent, we predict that pro-SISS-1 will trigger sleep only with a noxious heat shock. We incubated hs:pro-SISS-1 and hs:sec-SISS-1 animals, along with non-transgenic controls, for 30 min at either 29 °C or 35 °C and examined their subsequent sleep behavior. Following the 29 °C exposure, transgene-dependent sleep was observed in hs:sec-SISS-1 animals, confirming activation of the heat shock promoter at this temperature, but sleep was not observed in hs:pro-SISS-1 animals (Fig. 5d, f). By contrast, following a 35 °C exposure, endogenous SIS was observed as well as robust sleep from both transgenes (Fig. 5e, f). The dependence of pro-SISS-1 but not sec-SISS-1 sleep on the presence of noxious heat points to SISS-1 shedding as a stress-responsive event. Together our data suggest that ADM-4 is activated by certain forms of cellular damage, similar to ADAM17. Given the variety of noxious conditions that trigger SIS, including heat, UV light exposure, osmotic stress, wounding, and toxin ingestion, it is likely that ADM-4 is responsive to many types of cellular stress.

ADM-4 functions within damaged tissues

Damaging conditions with distinct tissue specificities can trigger stress-induced sleep. In particular, wounding the animal in the head, mid-body, or tail region can induce SIS[12], and ingestion of Cry5B toxin, which produces intestine-specific damage[41,42], is a potent SIS trigger. Moreover, noxious heat and UV exposure each induce SIS and are predicted to cause widespread damage. Given these observations, we reasoned that ADM-4 may function in a range of tissues to release SISS-1 from damaged cells, a model supported by the widespread and overlapping transcription patterns of ADM-4 and SISS-1[43]. In an alternative model, damaged cells might signal to a single hub of ADM-4-dependent SISS-1 release. To investigate these possibilities, we examined the tissue requirements for ADM-4, which unlike SISS-1 is predicted to function in a cell-autonomous manner. Using cGAL, a GAL4-UAS bipartite expression system optimized for *C. elegans*[44], we generated strains in which ADM-4 was expressed exclusively within one of each of the following tissues: the nervous system, epidermal tissue, pharyngeal muscle, body muscle, intestinal cells, and the ALA neuron itself (Supplementary Fig. 7). We then examined these strains for stress-induced sleep in response to two stressors: Cry5B toxin, which is known to cause intestine-specific damage, and UV-B irradiation, which we expect to cause widespread damage. We found that in response to Cry5B ingestion, ADM-4 expression in the intestine, but not in any other tissue, restores SIS to *adm-4* null mutant animals (Fig. 6a). By contrast, SIS triggered by UV-B irradiation is not rescued by intestinal ADM-4 expression, and instead we observe partial SIS rescue by ADM-4 expression within pharyngeal muscle or the epidermis (Fig. 6b). It is not known whether these *C. elegans* tissues are more sensitive to UV-B or simply better equipped to shed SISS-1. However, as the majority of UV-B damage to the vertebrate cornea occurs in the outermost layer of epithelium[45], the nematode epidermis may incur a large fraction of the damage from UV-B exposure. The distinct tissue requirements for ADM-4 in different forms of SIS support a model in which ADM-4 functions within damaged tissues to release SISS-1. These data complement recent studies showing that genetic disruption of proteostasis in peripheral tissues enhances EGFR-dependent sleep in *C. elegans*[8].

SISS-1 overexpression has limited effects on vulva development

Organogenesis of the *C. elegans* vulva depends on activation of the EGF receptor LET-23 in vulval precursor cells (VPCs) within the ventral epithelium during the second larval (L2) stage[46]. LIN-3 released from the gonadal anchor cell (AC) promotes vulval fates in three of six competent VPCs, with the nearest (P6.p) adopting a primary fate distinct from its neighbors (P5.p and P7.p), and the more distant VPCs (P3.p, P4.p and P8.p) remaining uninduced[17,47–49] (Fig. 7a). LIN-3 overexpression from multicopy arrays or from heat-inducible transgenes promotes hyperinduction, with up to six VPCs adopting vulval fates[17,49]. While *lin-3* mutants are defective in vulva development, *siss-*

https://doi.org/10.1038/s41467-024-55252-4

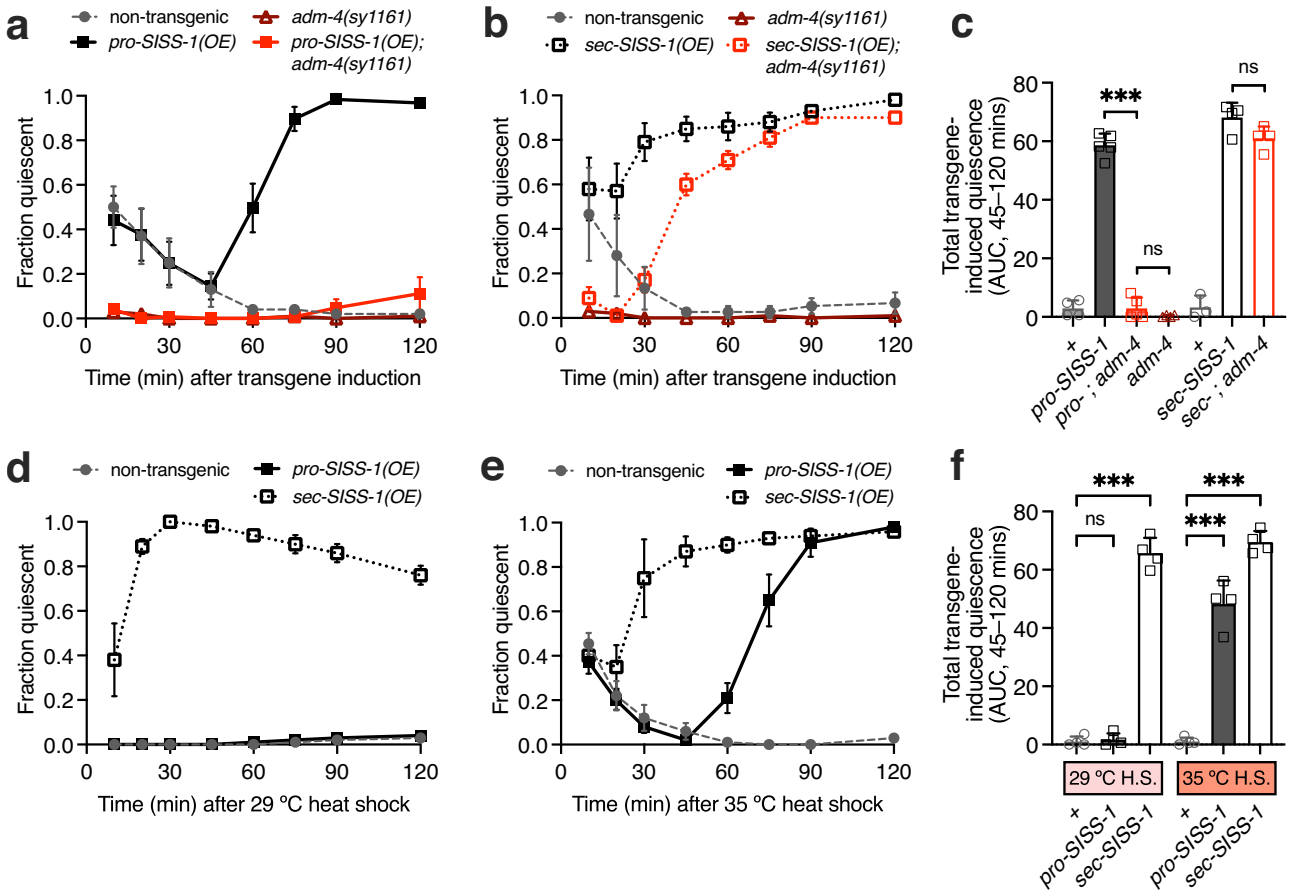

Fig. 5 | SISS-1 shedding is stress-responsive and depends on ADM-4. a Time-course of fraction quiescent *pro-SISS-1(OE) (csnEx1);* + (black trace), *pro-SISS-1(OE); adm-4(sy1161)* (red), *adm-4(sy1161)* (maroon), and non-transgenic (gray) animals following a 20-min 35 °C heat shock (h.s.) to induce expression of full-length *siss-1*. **b** Time-course of fraction quiescent *sec-SISS-1(OE) (csnEx2);* + (black trace), *sec-SISS-1(OE); adm-4(sy1161)* (red), *adm-4(sy1161)* (maroon), and non-transgenic (gray) animals following a 20-min 35 °C h.s. to induce expression of a constitutively secreted form of *siss-1*. **c** Total transgene-induced quiescence (area under curve (AUC), 45–120 min) for data shown in **a** and **b**. **d**–**e** Time course of fraction quiescent *pro-SISS-1(OE)* (black, closed squares), *sec-SISS-1(OE)* (black, open squares), and non-transgenic (gray, closed circles) animals: (**d**) following a 20-min 29 °C h.s. to induce expression of each transgene with minimal heat stress, or (**e**) following a 20-min 35 °C h.s. to induce expression of each transgene with heat stress. **f** Total transgene-induced quiescence (AUC, 45–120 min) for data shown in **d** and **e**. All AUC calculations exclude the first 45 minutes of the time course to distinguish transgene-induced quiescence from SIS induced by the heat shock. Each AUC data point represents one trial of 25 animals. All error bars represent SEM. ***$P < 0.0001$, ns = $P > 0.05$, One-way ANOVA with Tukey's multiple comparisons test. Source data are provided as a Source Data file.

1 mutants are not (Supplementary Fig. 1f), indicating that SISS-1 does not contribute to the endogenous inductive signal. However, given that overexpression of either ligand can promote sleep, we reasoned that ectopic expression of SISS-1 might promote excess vulval cell fates. Using the same heat-inducible transgenic lines as in our sleep experiments, we induced expression of each full-length ligand in a wild-type background at the L2 stage and examined vulva morphogenesis at the L4 stage. We observed highly penetrant hyperinduction of vulval fates with LIN-3(OE) (Fig. 7b), but not with SISS-1(OE) (Fig. 7c), even though these transgenes show similar effects on sleep (Figs. 3d and 4c). While the heat shock used to induce ubiquitous expression of these transgenes should be sufficient to activate ADM-4, we considered the possibility that SISS-1 shedding might be a limiting factor. We therefore examined overexpression of secreted SISS-1, and we observed mild hyperinduction in a small fraction of animals (Fig. 7d, e). Our finding that sec-SISS-1 can promote vulval fates at all is consistent with SISS-1 functioning as an EGFR ligand. However, the capacity of SISS-1 to impact vulval induction is weak compared to LIN-3, and weak relative to the impact of SISS-1 on sleep. These factors may contribute to the observed insulation of vulval induction from stress-induced sleep during development[15,49].

Discussion

We have identified SISS-1, a *C. elegans* EGF family ligand that appears to be shed from damaged tissues to activate sleep-promoting neurons (Fig. 8). This stress-induced sleep in turn promotes recovery from noxious conditions[9,13,50], indicating that sleep complements cell-autonomous repair processes. In mammals, ectodomain shedding of EGF family ligands occurs in response to a variety of stimuli including damaging conditions. For example, HB-EGF is shed from keratinocytes and corneal epithelial cells in response to wounding[51,52], TGF-alpha is shed from renal medullary cells exposed to osmotic stress[53], and amphiregulin is shed from skin cancer cell lines following UV irradiation[54] and from lung epithelial cells following exposure to tobacco smoke[37]. In these cases, EGF signaling is associated with wound healing, cell survival, or proliferation. In addition, EGF signaling is associated with sleep across phyla[55–59]. The connection between cellular stress and sleep is clear in *C. elegans*, where sleep is independent of circadian regulation and ensues rapidly following exposure to damaging conditions[9]. In other animals, signs of cellular stress within the brain and peripheral tissues accrue with wakefulness and dissipate with sleep[1–6], and we speculate that these tissues contribute to daily sleep pressure. Thus, stress-induced EGF signaling may contribute not

https://doi.org/10.1038/s41467-024-55252-4

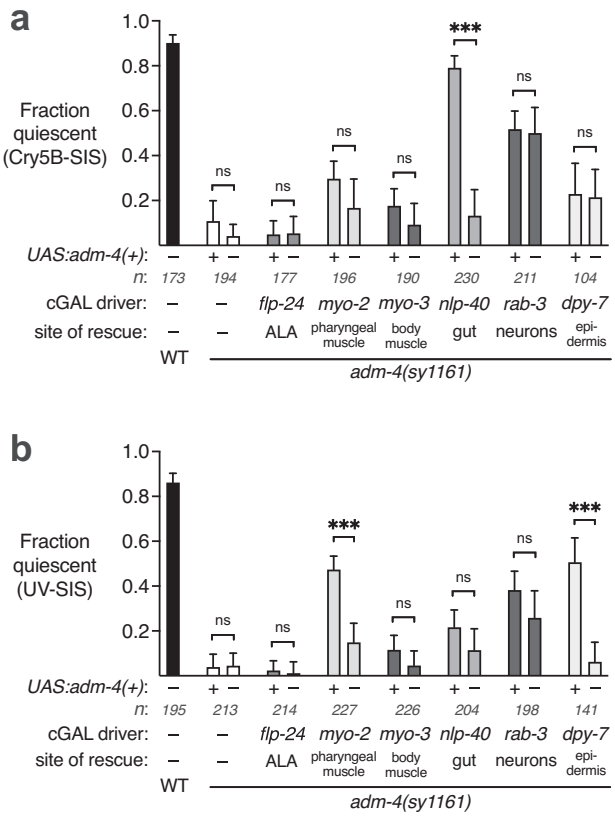

Fig. 6 | The spatial requirement for ADM-4 depends on the damaging agent. **a** Fraction of animals quiescent at a single time point between 10 and 20 min after a 10-min Cry5B exposure in wild type (WT), *adm-4(sy1161)*, and transgenic *adm-4(sy1161)* young adult animals in which a wild-type *adm-4(+)* is expressed in specific tissues using the cGAL expression system. The *rab-3:cGAL* line harbors a different *adm-4* CRISPR allele *(sy1837)*, which was generated directly in that line and appears to have some residual ADM-4 activity. **b** Same as in panel **a**, but at a single time point between 75 and 90 min after a 50-sec UV-B exposure. Animals were scored with experimenter blind to the presence of *UAS:adm-4(+)* and thus each trial varied in the number of animals of each genotype examined. For each strain, categorical data was collected across at least three independent trials of 20–50 animals per genotype. Error bars represent 95% confidence intervals. ***$P < 0.0001$, ns = $P > 0.05$, Fisher's exact test. Source data are provided as a Source Data file.

only to cell-autonomous repair and cell survival, but also to organismal sleep that enhances cellular repair.

Our work indicates that SISS-1 shedding requires the metalloprotease ADM-4. We find that ADM-4 is required for SIS, functions genetically upstream of EGFR, and is dispensable when SISS-1 lacks a membrane tether. Vertebrate ADAMs play roles in many physiological processes by promoting the shedding of a diverse array of signaling molecules, including EGFR ligands. Intriguingly, whereas mammalian EGFR ligands are primarily shed by ADAMs[20] and can be shed by the Rhomboid family proteases in some contexts[60,61], only the Rhomboids have been implicated in EGFR ligand processing in invertebrates[20,62]. To our knowledge, this study represents the first evidence of a role for ADAMs in invertebrate EGFR signaling, indicating that the interaction between ADAM proteases and EGFR ligands may have arisen earlier in evolution than previously thought.

We also find that SISS-1 shedding requires noxious conditions, suggesting that ADM-4 activation is stress-responsive. Consistent with this notion, ADM-4 also plays a role in axonal repair following injury[63]. How does ADM-4 integrate diverse noxious stimuli, including wounding, ingestion of pore-forming toxin, heat stress and UV irradiation? The ADM-4 ortholog ADAM17 is also activated by noxious stimuli[21,37] and is subject to multiple layers of regulation including trafficking by catalytically inactive Rhomboids (iRhoms), maturation by furin-like proprotein convertases, modulation by protein disulfide isomerases, interaction with integrins, stimulation by GPCR signaling, and responsiveness to membrane composition[64]. However, it is still not clear which intracellular pathways activate ADAM17 activity in response to stress. While the cytoplasmic domain of ADAM17 is subject to phosphorylation by p38 MAP kinases[65], which are known to be activated by a variety of stresses[66], the cytoplasmic domain of ADAM17 appears to be dispensable for its activation by physiological signals[67,68]. A close examination of ADM-4 may shed light not only on the regulation of *C. elegans* stress-induced sleep, but also on the physiological modes of ADAM17 activation, with implications for inflammatory responses and cancer.

Our work reveals that *C. elegans* has at least two functional EGFR ligands, LIN-3 and SISS-1. LIN-3 participates in developmentally-timed EGFR signaling events, and its transcription is under tight spatial and temporal control[43,69,70]. By contrast, SISS-1 is more broadly expressed[43] and is shed by a variety of tissues under stress to promote EGFR-dependent sleep, which can occur at any stage[15]. If these signaling events were not insulated, one might expect hyperinduction of vulval fates following exposure of wild-type larval animals to stress, which is not observed[15,49]. Widespread overexpression of either SISS-1 or LIN-3 can promote sleep, indicating that these ligands are somewhat interchangeable in the context of neuronal EGFR activation. However, SISS-1(OE) cannot phenocopy LIN-3(OE) in the induction of vulval cell fates, even though the inducible promoter used to drive expression of these ligands is active in most tissues, including vulval cells[40]. This difference is not attributable to regulated SISS-1 shedding, as even a constitutively secreted SISS-1 is a weak inducer of vulval fates. We speculate that the SISS-1 EGF domain has inherently low affinity for the receptor, like a subset of vertebrate EGFR ligands[71], and that the sleep neurons respond to a lower level of EGFR activation than do the vulval precursor cells. It is also possible that the SISS-1 immunoglobulin domain influences the activity of the ligand in a spatial manner. Notably, the immunoglobulin domain of vertebrate Neuregulin-1 confers enhanced and extended ErbB receptor activation[28], likely via anchoring of the ligand to heparan sulfate proteoglycans within the extracellular matrix (ECM)[72,73]. Accordingly, the disparate impact of SISS-1 on neuronal versus epithelial EGFR activation might reflect ECM differences between these tissues. The mechanism conferring insulation of developmental and behavioral EGFR signaling events is under investigation.

Methods

Strains and standard for all assays

Strains used in this study and their sources are listed in Supplementary Table 2. Worms were grown and maintained on nematode growth media (NGM) at 20 °C and fed OP50 *Escherichia coli* bacteria as a food source[74]. Pre-fertile young adults were examined for normal locomotion and feeding behavior prior to exposure to stressors described below. During SIS assays, all plates were kept on the stereomicroscope platform, and each plate was slid gently into the field of view 30 s prior to examination. Behavioral quiescence was scored with experimenter blind to genotype and was defined as a lack of both locomotion and pharyngeal pumping during a 4 s observation. An animal showing any movement or feeding was categorized as non-quiescent.

Heat-SIS and EGF(OE) sleep

Young adult animals were placed onto 35 × 10 mm (4 ml) NGM plates seeded with OP50 *E. coli* that were then sealed with parafilm and placed upright (lid up) in a heated circulating water bath. For heat-SIS assays, a 30-min 35 °C heat shock was used. To induce transgene expression for examination of EGF(OE) sleep, 20-min heat shocks at either 29 °C (transgene induction without SIS) or 35 °C (transgene induction with

https://doi.org/10.1038/s41467-024-55252-4

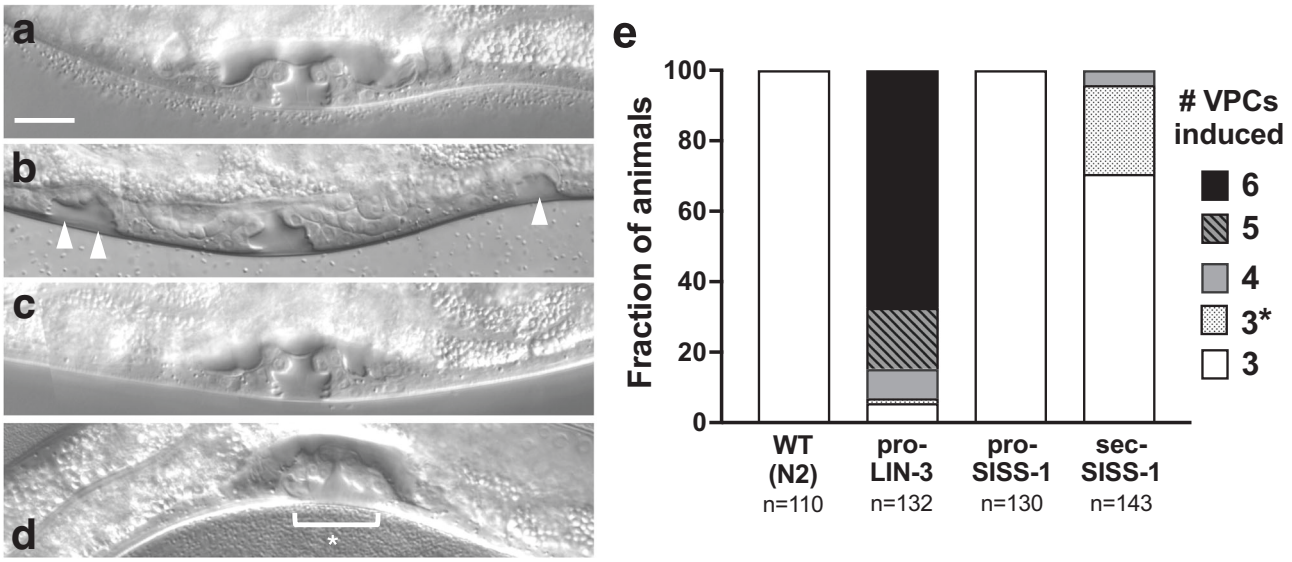

Fig. 7 | SISS-1 is a weak inducer of vulval cell fates. a–d Vulva morphogenesis at the L4 larval stage (anterior left, ventral down). Scale bar = 20 µm. All animals were heat-shocked at 33 °C for 20 min at the L2 stage to induce *lin-3* or *siss-1* overexpression in a wild-type background. **a** Heat-shocked wild-type animals show normal vulval morphology characteristic of graded induction of three vulval precursor cells (VPCs P5.p–P7.p). **b** Animals expressing pro-LIN-3 display additional vulval fates in P3.p, P4.p and P8.p (arrowheads). **c** Animals expressing pro-SISS-1 show no hyperinduction of vulval fates. **d** Expression of a constitutively secreted SISS-1 causes weak hyperinduction, shown here as an excess of primary-fated cells among P5.p-P7.p that detach from the ventral surface (bracket and asterisk). In a small fraction of sec-SISS-1 animals, an additional VPC is induced to adopt a vulval fate. **e** Number of VPCs induced, inferred by examination of vulval morphology at the L4 stage. Normally three VPCs are induced, with only P6.p adopting a primary fate. 3* represents animals with an excess of primary-fated cells among P5.p-P7.p, with no additional VPCs induced. Numbers at the base of each bar indicate how many animals of that genotype were examined. Source data are provided as a Source Data file.

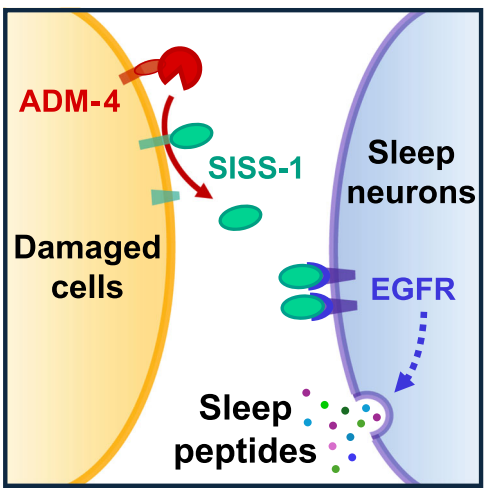

Fig. 8 | Model for stress-induced activation of sleep-promoting neurons. Our data support a model in which peripheral tissue damage leads to cell-autonomous activation of the metalloprotease ADM-4, which catalyzes ectodomain shedding of the Epidermal Growth Factor (EGF) family ligand SISS-1. SISS-1 in turn activates EGF receptors (EGFR) in the neurons ALA and RIS, leading to the release of neuropeptides that collectively bring about organismal sleep. Solid arrow = proteolysis; dotted arrow = signal transduction. Schematic created using Microsoft PowerPoint.

SIS) were used. After heat shock, plates were cooled to room temperature by placing on ice for 30 s–1 min, parafilm was removed and plates were moved to a stereomicroscope for examination of SIS and/or transgene-dependent sleep.

Cry5B-SIS

Young adult animals were placed onto NGM plates containing 60 ug/ml carbenicillin and 1 mM IPTG that had been seeded with JM103 bacteria harboring an IPTG-inducible Cry5B toxin[75]. Behavior was scored across time points in the presence of Cry5B for all Cry5B-SIS assays except the ADM-4 site of action analysis (Fig. 6) and protease gene RNAi (Supplementary Fig. 1), in which animals were exposed to Cry5B for 10 min, transferred to NGM 'detox' plates seeded with OP50 *E. coli*, and assayed for sleep 10 min later.

UV-SIS

Young adult animals were transferred to NGM plates seeded with OP50 *E. coli*. Plates were placed lid-down on a UVP M-10E mini benchtop 302 nm (UVB) 60 mW/cm^2 transilluminator gel box for 50 s and assayed for SIS. For each experiment, the same lid was used for all plates to control for potential variation in lid thickness.

Isolation of *siss-1(csn20)*

N2 animals were exposed to 50 mM ethylmethanesulfonate[74] and their F2 progeny were exposed to Cry5B for 10 min and screened for sleep defects. Candidate lines were subsequently screened for defects in UV-SIS and heat-SIS. Fully SIS-defective mutants were screened for intact LIN-3(OE) sleep, with the intention of isolating components upstream of EGFR activation. One mutant, *csn20*, fulfilled these criteria and was subjected to SNP mapping using a polymorphic Hawaiian strain of *C. elegans*. As the standard Hawaiian strain CB4856 contains a low activity variant of the *npr-1* gene that is associated with SIS defects[32] we used CX11400, containing the *npr-1* allele from N2 introgressed into the Hawaii genetic background[76], which shows SIS responses close to those of N2[32]. Genetic mapping placed the causative mutation just to the right of the centromere of chromosome IV, and whole-genome sequencing (BGI Genomics) revealed a Cys-to-Tyr substitution within the coding region of F28E10.2, initially named *igeg-1* for its immunoglobulin and EGF domains[18]. We subsequently named this locus *siss-1*.

EGF sequence analyses

EGF domain sequences were selected from four residues upstream of the first conserved cysteine to one residue after the sixth conserved

cysteine[26]. Pairwise sequence comparisons with SISS-1 were performed using the ebi.ac.uk EMBOSS NEEDLE tool[77] using the following parameters: output format = pair; matrix = BLOSUM62; gap open = 10; gap extend = 0.5; end gap = true; end gap open = 15; end gap extend = 0.5. For neuregulins 1 and 2, two isoforms arising from alternative splicing within the EGF domain (alpha and beta) were included. The two highest-scoring *H. sapiens* family members EGF and EREG, all four *D. melanogaster* members, and *C. elegans* LIN-3 were used for multiple sequence alignment (Fig. 2b). Alignment of the EGF domains of SISS-1 and selected EGFR ligands were generated with the MUSCLE alignment tool within SnapGene software (www.snapgene.com).

lin-3 strains and Cry5B resistance

lin-3(n1058) is a strong reduction of function allele that impairs viability, vulval induction and fertility[33] and can be maintained as a homozygote only in the presence of second site mutations that suppress the fertility defect[78]. Fertility is restored by the closely linked *itr-1(sy290gf)* mutation in PS1378 and by a *lfe-2(sy326)* mutation in PS1595. The PS1595 strain also harbors a *dpy-20* mutation that is closely linked to *lin-3*. The PS1378 strain shows a Cry5B resistance phenotype (failure to slow pharyngeal pumping in the presence of the toxin) that we were able to separate from the *lin-3 and itr-1* mutations by a single outcross to wild type N2 and subsequent screening for vulvaless Cry5B-sensitive recombinants, producing strain CVB80.

Transgene construction

Gene fragments from the first nucleotide of the F28E10.2b *siss-1* cDNA up to the EcoRV site of the 3'UTR were synthesized by Twist Biosciences with a KpnI site added to the 5' end. For the constitutively secreted sec-SISS-1 construct, only the extracellular region of the protein was included, and a synthetic signal peptide[35] was appended to the 5' end. Gene fragments were cloned KpnI-EcoRV into the heat-responsive *hsp-16* promoter vector pPD49.83 (Addgene plasmid #1448). Transgene sequences can be found within Source Data. Each construct was microinjected at 10 ng/ul into CVB11 *pha-1(e2123ts);him-5(e1490)* by InVivo Biosystems and outcrossed against N2 to establish CVB56 and CVB57.

RNA-mediated interference of candidate protease genes

Feeding RNAi was performed using the strain TU3335, in which the general RNAi response is enhanced by a mutation in *lin-15B* and neuronal RNAi is enhanced by expression of the SID-1 dsRNA transporter in the nervous system. Cultures of HT115 bacteria harboring a dsRNA clone (listed in Supplementary Fig. 1b) or an empty vector control (plasmid L4440) were plated onto NG plates containing 25 ug/ml carbenicillin and 1 mM IPTG and left at 37˚C overnight. The next day, TU3335 animals at the L4 stage were placed onto RNAi plates, incubated at 20˚C, and transferred each day to a new RNAi plate to create broods of progeny for multiple trials. Once progeny reached the young adult stage, they were examined for Cry5B-SIS as described above.

ADM-4 CRISPR alleles

The *sy1161* and *sy1837 adm-4* alleles were generated using the CRISPR-based STOP-IN strategy[23]. Briefly, a universal cassette, which contains an early STOP codon and causes a frame shift in all three reading frames, was inserted near the 5' end of the *adm-4* gene using CRISPR/Cas9 and homology-directed repair. The CRISPR guide RNAs were designed to target the following genomic sequence: GAAAGTTGATGCGGGTAAGA. The ~35-bp sequences flanking the universal STOP-IN cassette that, all together, comprise the HDR template are as follows: CTTTGTTGATGACACGTTACATCTAGAGCCATCT (left) and TACCCGCATCAACTTTCTGATGATCTTGGGCCTGTTG (right). The primers used to genotype *sy1161* and *sy1837* animals were: TGTGAAACGACATGCACCAATC (forward) and AACGAGTAATCGGCCACGAG (reverse).

ADM-4 site of action

For *adm-4* site-of-action experiments, we used the cGAL-UAS system[44] to drive expression of wild-type *adm-4* cDNA in specific tissues of *adm-4(lf)* animals. Strains containing an integrated or extrachromosomal tissue-specific cGAL driver (Supplementary Table S2) were each crossed to PS7951 *adm-4(sy1161)* animals. Because all available pan-neuronal drivers (*rab-3p:cGAL*) are integrated on the X chromosome, where the *adm-4* gene is located, *adm-4* was knocked out within the *rab-3p:cGAL* line PS6961 using the STOP-IN CRISPR strategy described above, yielding the *adm-4* allele *sy1837*. The UAS:adm-4(+):SL2:GFP transgene was constructed by amplifying the *adm-4* coding sequence from N2 cDNA using primers oHW541F: 5' - cccttggctagcgtcgacggtaccggtaaaaATGAAGATACAGGACAGATC - 3' and oHW542R: 5' - gaaagtaggatgagacagctacggtaccCTAATTGACGTCCGCTTTGAC - 3'. Coding sequences are capitalized and KpnI sites used for cloning are underlined. The amplified *adm-4* coding sequence was ligated to KpnI-digested pJL046[44] (Addgene plasmid #198807) by Gibson Assembly such that the *adm-4* coding sequence is positioned 3' to the 15X UAS and 5' to the SL2:GFP. The *UAS:adm-4(+)* effector line CVB91 was generated by injecting UAS:adm-4(+):SL2:GFP plasmid into PS7951 *adm-4(sy1161)* mutants. Each *adm-4* mutant cGAL driver line was crossed to CVB91 *UAS:adm-4(+); adm-4(sy1161)* to generate 'rescue' strains with *adm-4* expressed in specific tissue types. For each rescue strain, animals were subjected to UV-B and Cry5B conditions as described above and scored at a single time point for sleep. For UV-SIS, animals were scored between 60 and 90 min after a 50-s UV-B exposure. For Cry5B-SIS, animals were exposed to Cry5B for 10 min, transferred to regular OP50 *E. coli*, and then examined between 10 and 20 min later for sleep. Each animal was scored for sleep blind to transgene status under brightfield-only on a Leica M165 FC stereomicroscope, and the fluorescence shutter was then opened to distinguish driver-only from *adm-4(+)* rescued animals.

Vulva induction

Animals were heat shocked as above but at the late L2 stage for 30 min at 33 °C. This condition is sufficient to promote stress-induced sleep as well as transgene expression and produces less of a developmental delay relative to a 35 °C heat shock. This delay has been shown to be due to a prolonged cessation of feeding during EGF(OE)-induced sleep during larval stages[15]. Animals were examined at the L4 stage by differential interference contrast (DIC) microscopy on a Zeiss Axioimager A2 for invaginations of the ventral epithelium indicative of VPC induction.

Statistics and reproducibility

Statistical tests, indicated in figure legends, were performed using GraphPad Prism software (www.graphpad.com). All P values are two-sided, and significance was inferred at $P < 0.05$. To ensure reproducibility, data was typically generated from three biological replicates of 25 animals each, with the investigator blind to genotype during experiments and outcome assessment. No statistical method was used to predetermine sample size. SIS assays in which wild-type control animals did not show a fraction-quiescent peak of at least 0.25 were pre-established to be excluded from the study. This occurred occasionally in the case of heat-SIS, which is less replicable than other SIS types.

Reporting summary

Further information on research design is available in the Nature Portfolio Reporting Summary linked to this article.

Data availability

All data generated or analyzed in this study are included in the manuscript and Supplementary Information. Source data are provided with this paper.

References

1. Cirelli, C. & Tononi, G. Gene expression in the brain across the sleep-waking cycle. *Brain Res.* **885**, 303–321 (2000).
2. Naidoo, N., Giang, W., Galante, R. J. & Pack, A. I. Sleep deprivation induces the unfolded protein response in mouse cerebral cortex. *J. Neurochem.* **92**, 1150–1157 (2005).
3. Anafi, R. C. et al. Sleep is not just for the brain: transcriptional responses to sleep in peripheral tissues. *BMC Genomics* **14**, 362 (2013).
4. Everson, C. A., Henchen, C. J., Szabo, A. & Hogg, N. Cell injury and repair resulting from sleep loss and sleep recovery in laboratory rats. *Sleep* **37**, 1929–1940 (2014).
5. Bellesi, M., Bushey, D., Chini, M., Tononi, G. & Cirelli, C. Contribution of sleep to the repair of neuronal DNA double-strand breaks: evidence from flies and mice. *Sci. Rep.* **6**, 36804 (2016).
6. Zada, D., Bronshtein, I., Lerer-Goldshtein, T., Garini, Y. & Appelbaum, L. Sleep increases chromosome dynamics to enable reduction of accumulating DNA damage in single neurons. *Nat. Commun.* **10**, 895 (2019).
7. Williams, J. A. & Naidoo, N. Sleep and Cellular Stress. *Curr. Opin. Physiol.* **15**, 104–110 (2020).
8. Kawano, T. et al. ER proteostasis regulators cell-non-autonomously control sleep. *Cell Rep.* **42**, 112267 (2023).
9. Hill, A. J., Mansfield, R., Lopez, J. M. N. G., Raizen, D. M. & Van Buskirk, C. Cellular stress induces a protective sleep-like state in C. elegans. *Curr. Biol. CB* **24**, 2399–2405 (2014).
10. Nelson, M. D. et al. FMRFamide-like FLP-13 neuropeptides promote quiescence following heat stress in Caenorhabditis elegans. *Curr. Biol. CB* **24**, 2406–2410 (2014).
11. DeBardeleben, H. K., Lopes, L. E., Nessel, M. P. & Raizen, D. M. Stress-Induced Sleep After Exposure to Ultraviolet Light Is Promoted by p53 in Caenorhabditis elegans. *Genetics* **207**, 571–582 (2017).
12. Goetting, D. L., Mansfield, R., Soto, R. & Buskirk, C. V. Cellular damage, including wounding, drives C. elegans stress-induced sleep. *J. Neurogenet.* **34**, 430–439 (2020).
13. Konietzka, J. et al. Epidermal Growth Factor Signaling Promotes Sleep through a Combined Series and Parallel Neural Circuit. *Curr. Biol. CB* **30**, 1–16.e13 (2020).
14. Nath, R. D., Chow, E. S., Wang, H., Schwarz, E. M. & Sternberg, P. W. C. elegans Stress-Induced Sleep Emerges from the Collective Action of Multiple Neuropeptides. *Curr. Biol. CB* **26**, 2446–2455 (2016).
15. Van Buskirk, C. & Sternberg, P. W. Epidermal growth factor signaling induces behavioral quiescence in Caenorhabditis elegans. *Nat. Neurosci.* **10**, 1300–1307 (2007).
16. Harris, R. C., Chung, E. & Coffey, R. J. EGF receptor ligands. *Exp. Cell Res.* **284**, 2–13 (2003).
17. Hill, R. J. & Sternberg, P. W. The gene lin-3 encodes an inductive signal for vulval development in C. elegans. *Nature* **358**, 470–476 (1992).
18. Sternberg, P. W. et al. WormBase 2024: status and transitioning to Alliance infrastructure. *Genetics* **227**, iyae050 (2024).
19. Freeman, M. The rhomboid-like superfamily: molecular mechanisms and biological roles. *Annu. Rev. Cell Dev. Biol.* **30**, 235–254 (2014).
20. Blobel, C. P. ADAMs: key components in EGFR signalling and development. *Nat. Rev. Mol. Cell Biol.* **6**, 32–43 (2005).
21. Fischer, O. M., Hart, S., Gschwind, A., Prenzel, N. & Ullrich, A. Oxidative and osmotic stress signaling in tumor cells is mediated by ADAM proteases and heparin-binding epidermal growth factor. *Mol. Cell. Biol.* **24**, 5172–5183 (2004).
22. Gooz, M. ADAM-17: the enzyme that does it all. *Crit. Rev. Biochem. Mol. Biol.* **45**, 146–169 (2010).
23. Wang, H., Park, H., Liu, J. & Sternberg, P. W. An Efficient Genome Editing Strategy To Generate Putative Null Mutants in Caenorhabditis elegans Using CRISPR/Cas9. *G3 Bethesda Md* **8**, 3607–3616 (2018).
24. Van Buskirk, C. & Sternberg, P. W. Paired and LIM class homeodomain proteins coordinate differentiation of the C. elegans ALA neuron. *Dev. Camb. Engl.* **137**, 2065–2074 (2010).
25. Jarriault, S. & Greenwald, I. Evidence for functional redundancy between C. elegans ADAM proteins SUP-17/Kuzbanian and ADM-4/TACE. *Dev. Biol.* **287**, 1–10 (2005).
26. UniProt Consortium. UniProt: the Universal Protein Knowledgebase in 2023. *Nucleic Acids Res.* **51**, D523–D531 (2023).
27. Stein, R. A. & Staros, J. V. Insights into the evolution of the ErbB receptor family and their ligands from sequence analysis. *BMC Evol. Biol.* **6**, 79 (2006).
28. Donaldson, T. et al. Regulation of the Drosophila epidermal growth factor-ligand vein is mediated by multiple domains. *Genetics* **167**, 687–698 (2004).
29. Li, Q. & Loeb, J. A. Neuregulin-heparan-sulfate proteoglycan interactions produce sustained erbB receptor activation required for the induction of acetylcholine receptors in muscle. *J. Biol. Chem.* **276**, 38068–38075 (2001).
30. Falls, D. L. Neuregulins: functions, forms, and signaling strategies. *Exp. Cell Res.* **284**, 14–30 (2003).
31. Au, V. et al. CRISPR/Cas9 Methodology for the Generation of Knockout Deletions in Caenorhabditis elegans. *G3 Bethesda Md* **9**, 135–144 (2019).
32. Soto, R., Goetting, D. L. & Van Buskirk, C. NPR-1 Modulates Plasticity in C. elegans Stress-Induced Sleep. *iScience* **19**, 1037–1047 (2019).
33. Ferguson, E. L. & Horvitz, H. R. Identification and characterization of 22 genes that affect the vulval cell lineages of the nematode Caenorhabditis elegans. *Genetics* **110**, 17–72 (1985).
34. Turek, M., Lewandrowski, I. & Bringmann, H. An AP2 transcription factor is required for a sleep-active neuron to induce sleep-like quiescence in C. elegans. *Curr. Biol. CB* **23**, 2215–2223 (2013).
35. Perry, M. D. et al. Molecular characterization of the her-1 gene suggests a direct role in cell signaling during Caenorhabditis elegans sex determination. *Genes Dev.* **7**, 216–228 (1993).
36. Zunke, F. & Rose-John, S. The shedding protease ADAM17: Physiology and pathophysiology. *Biochim. Biophys. Acta Mol. Cell Res.* **1864**, 2059–2070 (2017).
37. Lemjabbar, H. et al. Tobacco smoke-induced lung cell proliferation mediated by tumor necrosis factor alpha-converting enzyme and amphiregulin. *J. Biol. Chem.* **278**, 26202–26207 (2003).
38. Brill, A. et al. Oxidative stress activates ADAM17/TACE and induces its target receptor shedding in platelets in a p38-dependent fashion. *Cardiovasc. Res.* **84**, 137–144 (2009).
39. Yin, J. & Yu, F.-S. X. ERK1/2 mediate wounding- and G-protein-coupled receptor ligands-induced EGFR activation via regulating ADAM17 and HB-EGF shedding. *Invest. Ophthalmol. Vis. Sci.* **50**, 132–139 (2009).
40. Stringham, E. G., Dixon, D. K., Jones, D. & Candido, E. P. Temporal and spatial expression patterns of the small heat shock (hsp16) genes in transgenic Caenorhabditis elegans. *Mol. Biol. Cell* **3**, 221–233 (1992).
41. Marroquin, L. D., Elyassnia, D., Griffitts, J. S., Feitelson, J. S. & Aroian, R. V. Bacillus thuringiensis (Bt) toxin susceptibility and isolation of resistance mutants in the nematode Caenorhabditis elegans. *Genetics* **155**, 1693–1699 (2000).
42. Griffitts, J. S., Whitacre, J. L., Stevens, D. E. & Aroian, R. V. Bt toxin resistance from loss of a putative carbohydrate-modifying enzyme. *Science* **293**, 860–864 (2001).

43. Taylor, S. R. et al. Molecular topography of an entire nervous system. *Cell* **184**, 4329–4347.e23, (2021).
44. Wang, H. et al. cGAL, a temperature-robust GAL4-UAS system for Caenorhabditis elegans. *Nat. Methods* **14**, 145–148 (2017).
45. Volatier, T. et al. Short-Term UVB Irradiation Leads to Persistent DNA Damage in Limbal Epithelial Stem Cells, Partially Reversed by DNA Repairing Enzymes. *Biology* **12**, 265 (2023).
46. Wang, M. & Sternberg, P. W. Pattern formation during C. elegans vulval induction. *Curr. Top. Dev. Biol.* **51**, 189–220 (2001).
47. Kimble, J. Alterations in cell lineage following laser ablation of cells in the somatic gonad of Caenorhabditis elegans. *Dev. Biol.* **87**, 286–300 (1981).
48. Sternberg, P. W. & Horvitz, H. R. Pattern formation during vulval development in C. elegans. *Cell* **44**, 761–772 (1986).
49. Katz, W. S., Hill, R. J., Clandinin, T. R. & Sternberg, P. W. Different levels of the C. elegans growth factor LIN-3 promote distinct vulval precursor fates. *Cell* **82**, 297–307 (1995).
50. Goetting, D. L., Soto, R. & Van Buskirk, C. Food-Dependent Plasticity in Caenorhabditis elegans Stress-Induced Sleep Is Mediated by TOR-FOXA and TGF-β Signaling. *Genetics* **209**, 1183–1195 (2018).
51. Tokumaru, S. et al. Ectodomain shedding of epidermal growth factor receptor ligands is required for keratinocyte migration in cutaneous wound healing. *J. Cell Biol.* **151**, 209–220 (2000).
52. Xu, K.-P., Ding, Y., Ling, J., Dong, Z. & Yu, F.-S. X. Wound-induced HB-EGF ectodomain shedding and EGFR activation in corneal epithelial cells. *Invest. Ophthalmol. Vis. Sci.* **45**, 813–820 (2004).
53. Küper, C., Bartels, H., Fraek, M.-L., Beck, F. X. & Neuhofer, W. Ectodomain shedding of pro-TGF-alpha is required for COX-2 induction and cell survival in renal medullary cells exposed to osmotic stress. *Am. J. Physiol. Cell Physiol.* **293**, C1971–C1982 (2007).
54. Singh, B., Schneider, M., Knyazev, P. & Ullrich, A. UV-induced EGFR signal transactivation is dependent on proligand shedding by activated metalloproteases in skin cancer cell lines. *Int. J. Cancer* **124**, 531–539 (2009).
55. Kushikata, T., Fang, J., Chen, Z., Wang, Y. & Krueger, J. M. Epidermal growth factor enhances spontaneous sleep in rabbits. *Am. J. Physiol.* **275**, R509–R514 (1998).
56. Kramer, A. et al. Regulation of daily locomotor activity and sleep by hypothalamic EGF receptor signaling. *Science* **294**, 2511–2515 (2001).
57. Snodgrass-Belt, P., Gilbert, J. L. & Davis, F. C. Central administration of transforming growth factor-alpha and neuregulin-1 suppress active behaviors and cause weight loss in hamsters. *Brain Res.* **1038**, 171–182 (2005).
58. Foltenyi, K., Greenspan, R. J. & Newport, J. W. Activation of EGFR and ERK by rhomboid signaling regulates the consolidation and maintenance of sleep in Drosophila. *Nat. Neurosci.* **10**, 1160–1167 (2007).
59. Lee, D. A. et al. Evolutionarily conserved regulation of sleep by epidermal growth factor receptor signaling. *Sci. Adv.* **5**, eaax4249 (2019).
60. Adrain, C. et al. Mammalian EGF receptor activation by the rhomboid protease RHBDL2. *EMBO Rep.* **12**, 421–427 (2011).
61. Urban, S., Schlieper, D. & Freeman, M. Conservation of intramembrane proteolytic activity and substrate specificity in prokaryotic and eukaryotic rhomboids. *Curr. Biol. CB* **12**, 1507–1512 (2002).
62. Dutt, A., Canevascini, S., Froehli-Hoier, E. & Hajnal, A. EGF signal propagation during C. elegans vulval development mediated by ROM-1 rhomboid. *PLoS Biol.* **2**, e334 (2004).
63. Ho, X. Y., Coakley, S., Amor, R., Anggono, V. & Hilliard, M. A. The metalloprotease ADM-4/ADAM17 promotes axonal repair. *Sci. Adv.* **8**, eabm2882 (2022).
64. Düsterhöft, S., Lokau, J. & Garbers, C. The metalloprotease ADAM17 in inflammation and cancer. *Pathol. Res. Pract.* **215**, 152410 (2019).
65. Xu, P. & Derynck, R. Direct activation of TACE-mediated ectodomain shedding by p38 MAP kinase regulates EGF receptor-dependent cell proliferation. *Mol. Cell* **37**, 551–566 (2010).
66. Coulthard, L. R., White, D. E., Jones, D. L., McDermott, M. F. & Burchill, S. A. p38(MAPK): stress responses from molecular mechanisms to therapeutics. *Trends Mol. Med.* **15**, 369–379 (2009).
67. Gall, L. et al. ADAM17 is regulated by a rapid and reversible mechanism that controls access to its catalytic site. *J. Cell Sci.* **123**, 3913–3922 (2010).
68. Schwarz, J. et al. Short-term TNFα shedding is independent of cytoplasmic phosphorylation or furin cleavage of ADAM17. *Biochim. Biophys. Acta BBA Mol. Cell Res.* **1833**, 3355–3367 (2013).
69. Hwang, B. J. & Sternberg, P. W. A cell-specific enhancer that specifies lin-3 expression in the C. elegans anchor cell for vulval development. *Dev. Camb. Engl.* **131**, 143–151 (2004).
70. Saffer, A. M., Kim, D. H., van Oudenaarden, A. & Horvitz, H. R. The Caenorhabditis elegans synthetic multivulva genes prevent ras pathway activation by tightly repressing global ectopic expression of lin-3 EGF. *PLoS Genet.* **7**, e1002418 (2011).
71. Singh, B., Carpenter, G. & Coffey, R. J. EGF receptor ligands: recent advances. *F1000Research* **5**, F1000 Faculty Rev-2270 (2016).
72. Loeb, J. A. & Fischbach, G. D. ARIA can be released from extracellular matrix through cleavage of a heparin-binding domain. *J. Cell Biol.* **130**, 127–135 (1995).
73. Meier, T. et al. Agrin can mediate acetylcholine receptor gene expression in muscle by aggregation of muscle-derived neuregulins. *J. Cell Biol.* **141**, 715–726 (1998).
74. Brenner, S. The genetics of Caenorhabditis elegans. *Genetics* **77**, 71–94 (1974).
75. Wei, J.-Z. et al. Bacillus thuringiensis crystal proteins that target nematodes. *Proc. Natl Acad. Sci. USA* **100**, 2760–2765 (2003).
76. Bendesky, A. *Genetic Variation in Neurotransmitter Receptors Generates Behavioral Diversity* (Rockefeller, 2012).
77. Madeira, F. et al. Search and sequence analysis tools services from EMBL-EBI in 2022. *Nucleic Acids Res.* **50**, W276–W279 (2022).
78. Clandinin, T. R., DeModena, J. A. & Sternberg, P. W. Inositol trisphosphate mediates a RAS-independent response to LET-23 receptor tyrosine kinase activation in C. elegans. *Cell* **92**, 523–533 (1998).

Acknowledgements

We thank Desiree Goetting and Trudi Schüpbach for critical reading of the manuscript, Virginia Vandergon for assistance with MSA analyses, and Carl Blobel and members of the Van Buskirk lab for helpful discussions. Thanks to members of the Sternberg lab for strain generation: Han Wang, Stephanie Nava, Wilber Palma and Shahla Gharib for production of *dpy-7p:cGAL* and UAS:*adm-4(+)* lines, and Heenam Park for generation of *adm-4* alleles *sy1161* and *sy1837*. We thank the *C. elegans* gene knockout consortium for generation of the *siss-1(ve532)* deletion. Many of the strains used in this study were provided by the Caenorhabditis Genetics Center, supported by the National Institutes of Health - Office of Research Infrastructure Programs (P40 OD010440). This work was supported by grants from the National Science Foundation (IOS 1553673 to C.V.) and the National Institutes of Health (R16 NS134541 to C.V. and R24 OD023041 to P.W.S.).

Author contributions

A.J.H. designed and performed experiments, analyzed the data, created figures, and drafted parts of the manuscript. B.R. isolated *siss-1(csn20)* and performed the initial characterization of the mutant. J.G.J. performed EGF domain sequence analyses and edited the manuscript. P.W.S. financed and supervised the production of cGAL and *adm-4* mutant strains and edited the manuscript. C.V. financed and supervised the project, designed and performed some of the experiments, and drafted parts of the manuscript.

Competing interests
The authors declare no competing interests.

Additional information
Supplementary information The online version contains supplementary material available at https://doi.org/10.1038/s41467-024-55252-4.

Correspondence and requests for materials should be addressed to Cheryl Van Buskirk.

Peer review information *Nature Communications* thanks Henrik Bringmann, and the other, anonymous, reviewer(s) for their contribution to the peer review of this work. A peer review file is available.